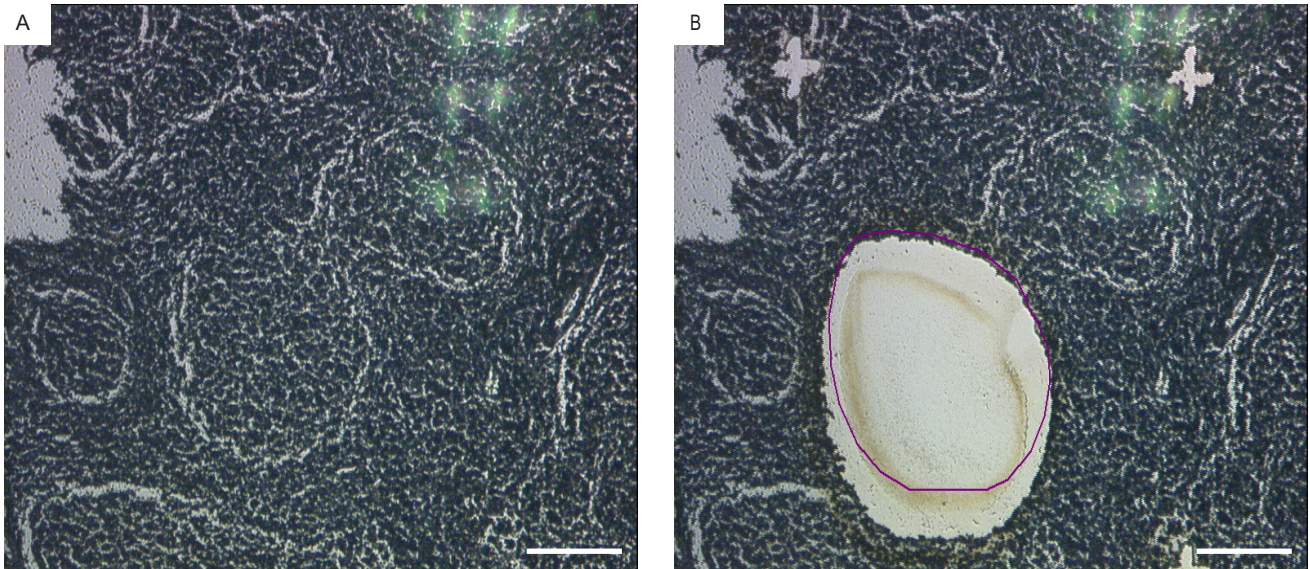
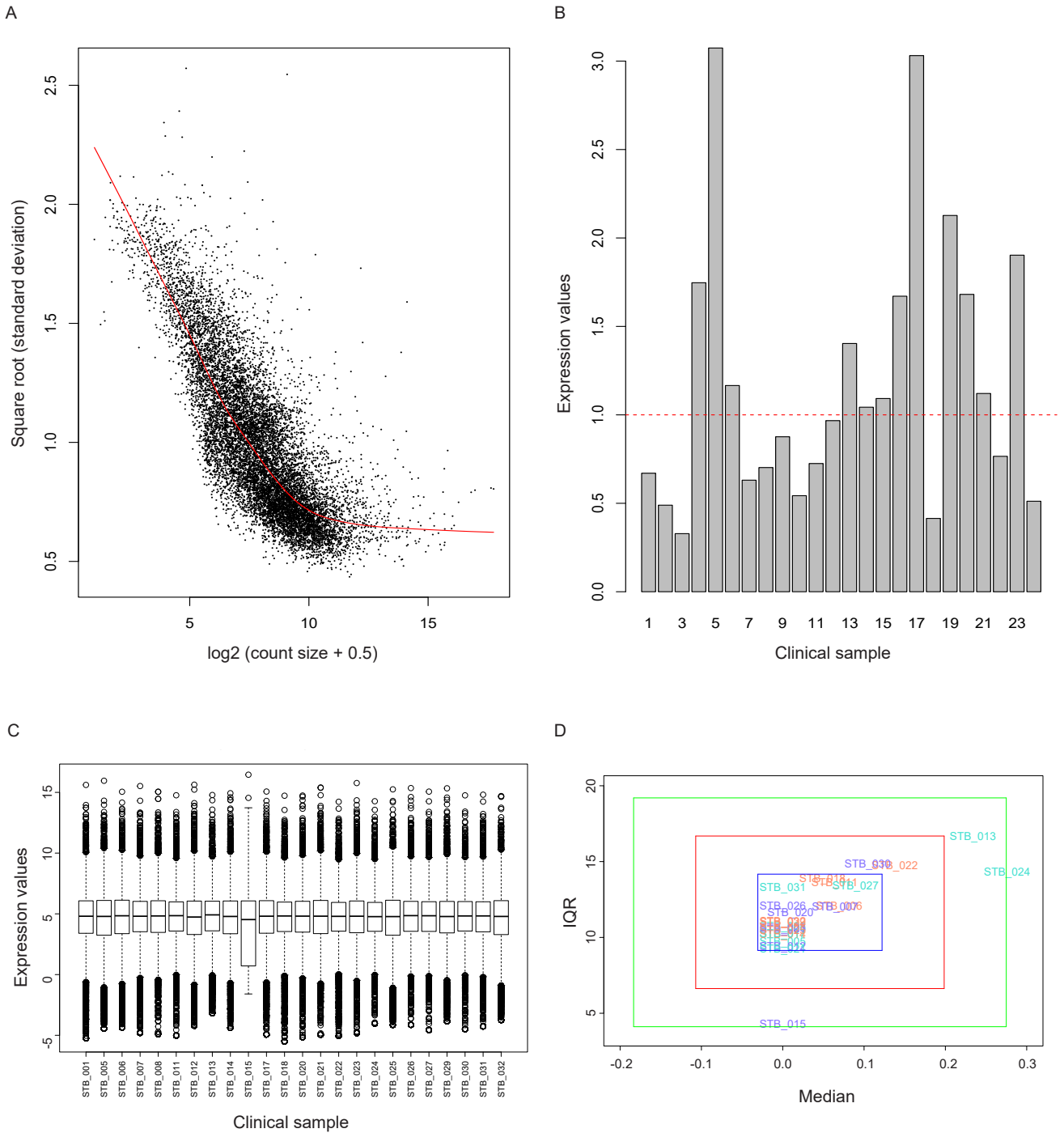


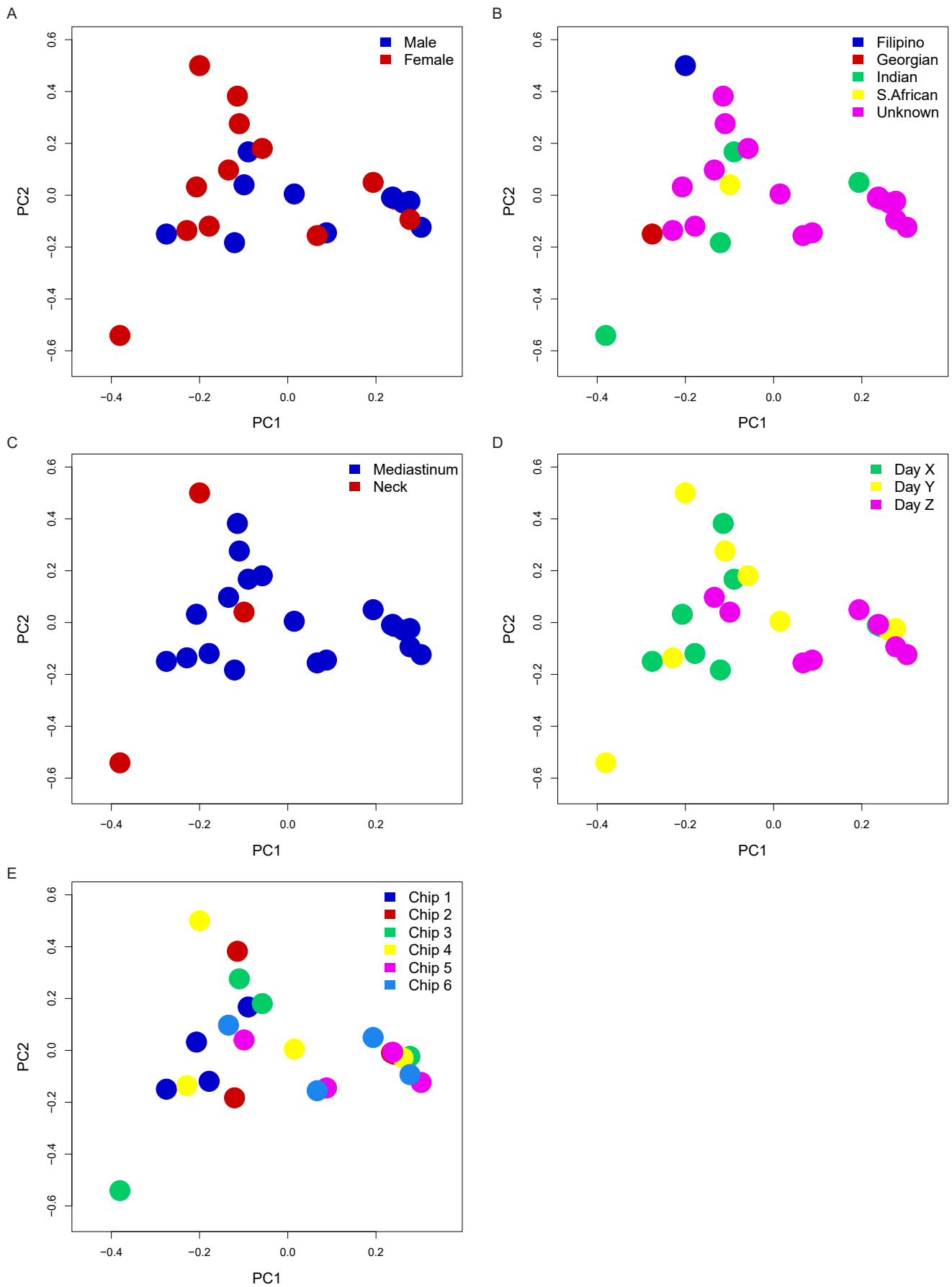
Supplemental Figure 1: Protocol for selection of biopsy specimens. The Southampton Biomedical Research Centre histology archive was searched to identify biopsies from tuberculosis (TB) lymph nodes, sarcoidosis lymph nodes and normal lymph nodes for a period between 2011 and 2016. Once the initial potential biopsies were identified, a series of screening steps were then performed to ensure definitive diagnosis, consistent age, consistent time since the biopsy was taken, absence of confounding clinical factors and availability of biopsy specimens. RNA was then extracted from eleven samples from each group, followed by sequencing of seven TB, ten sarcoidosis and seven normal lymph nodes.



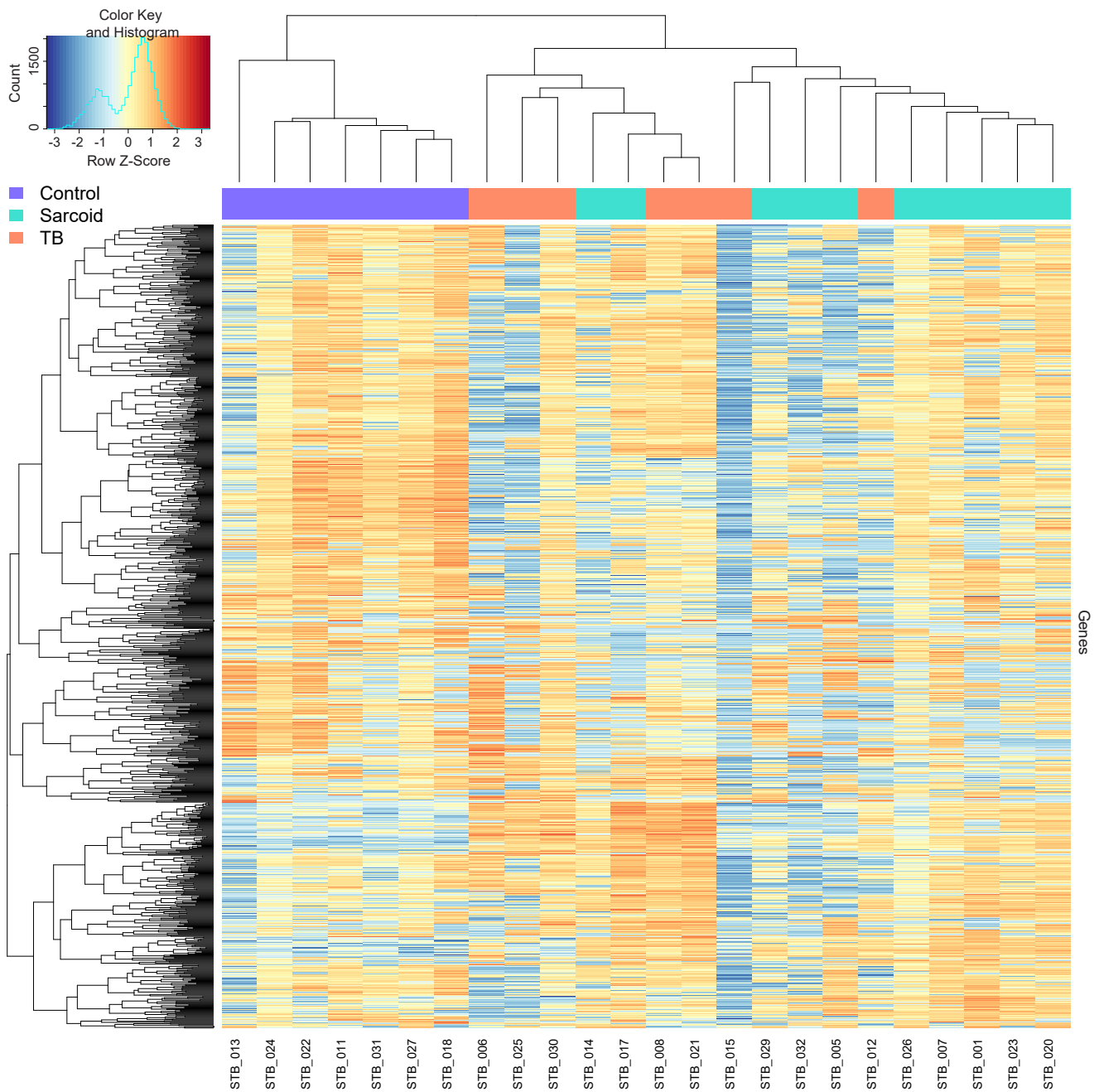
Supplemental Figure 2: Representative laser capture microdissection image. **A)** Appearance of unstained granulomas before laser capture. **B)** Section after granuloma capture. For each biopsy, an area of 8.0-8.19mm² was captured (mean 8.09mm²). Scale bars 200µm.



Supplemental Figure 3: Variance and normalization of lymph node RNAseq data. **A)** Mean variance trend following voom transformation shows appropriate filtering of raw counts. **B)** Sample specific weights across all samples generated by voom transformation. **C)** Median expression value is similar across all samples after TMM normalization and voom transformation. **D)** No samples are identified as outliers on plotting interquartile range against the median (TMM normalized) where 1 (blue), 2 (red), and 3 (green) standard deviation thresholds are used.

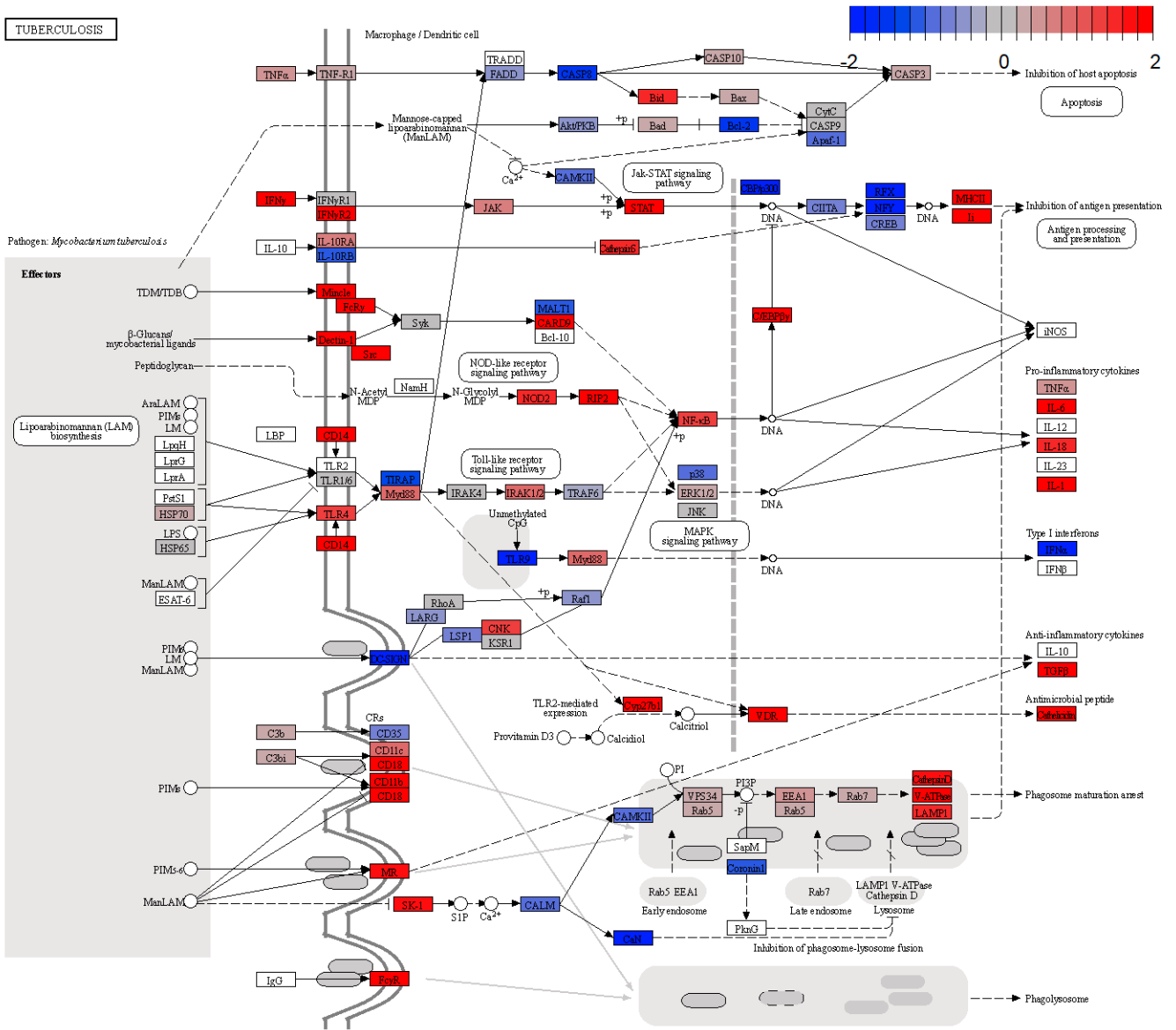


Supplemental Figure 4: Principle Component Analysis of potential confounding factors. PCA was plotted according to alternative variables to the diagnosis. PCA plots show no distinct clustering according to **A)** Gender, **B)** Ethnicity, **C)** Site of lymph node, **D)** Day of sequencing, or **E)** Sequencing chip.



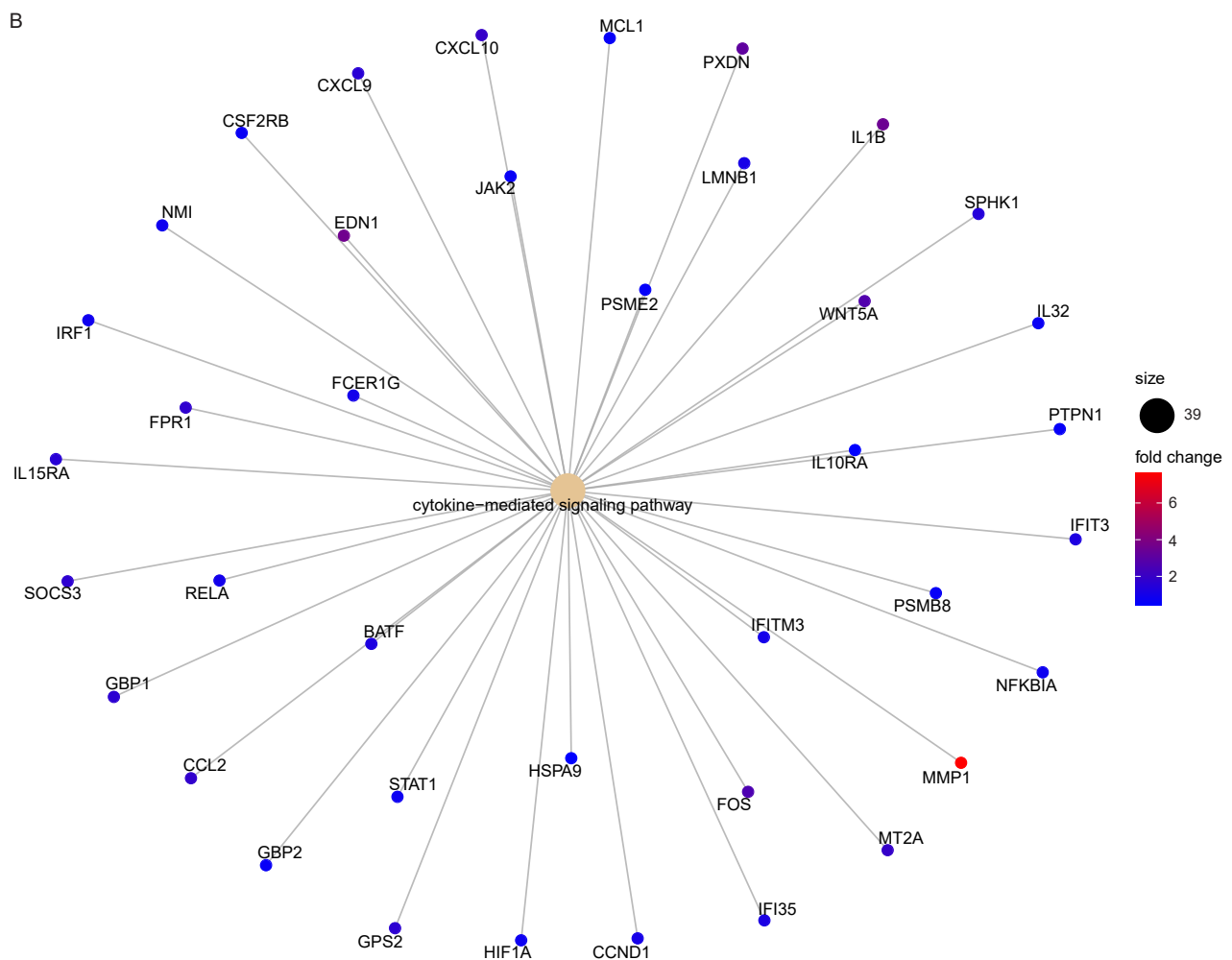
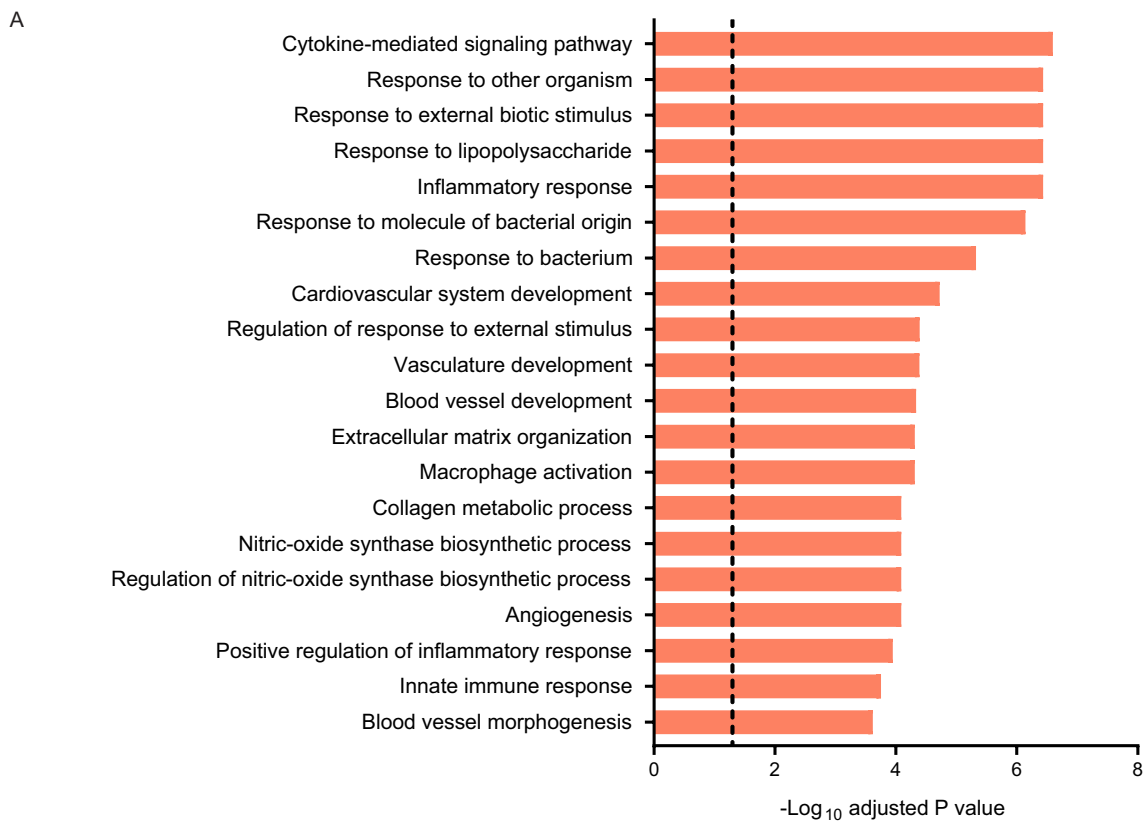
Supplemental Figure 5: Heat map and clustering according to top one thousand most variable genes. Hierarchical clustering was performed using the top one thousand most variable genes in the lymph node biopsies, using Spearman correlation and complete linkage. Consistent grouping of the control samples occurred, while no separation of the TB and sarcoidosis samples was observed.

TUBERCULOSIS



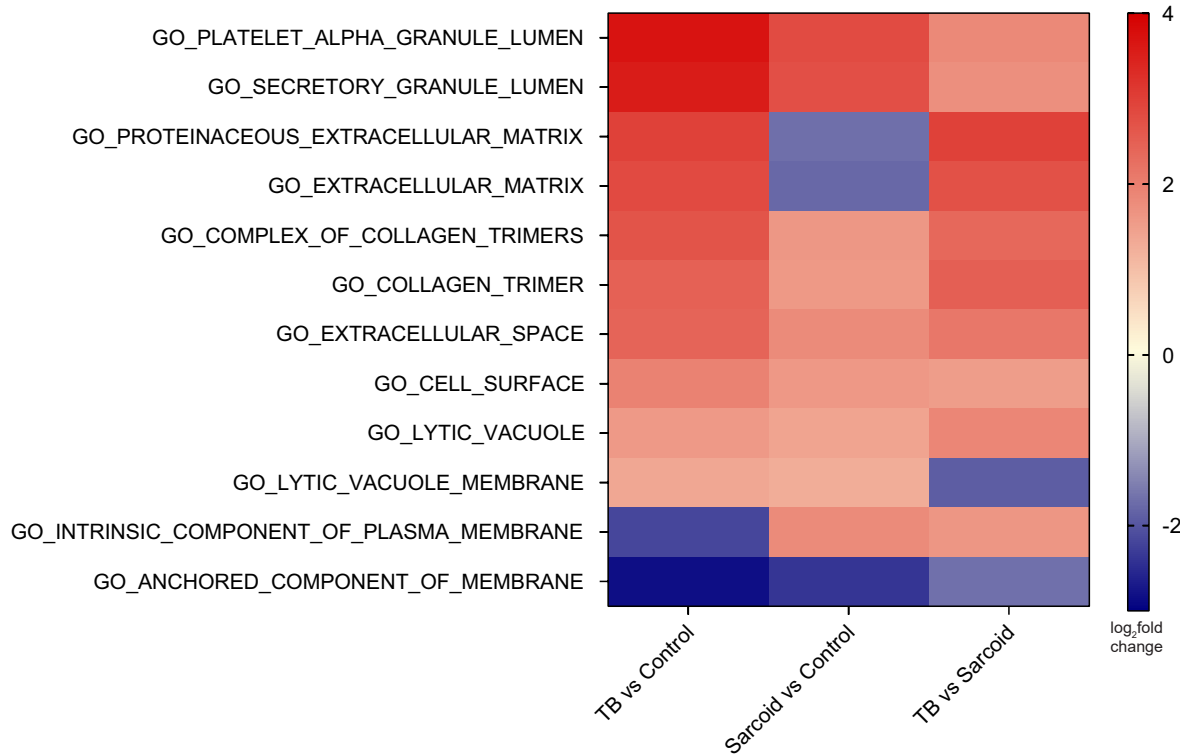
Rendered by Pathview

Supplemental Figure 6: Expression of genes regulated in clinical TB specimens overlaid on the KEGG TB pathway. Gene set enrichment analysis demonstrates a majority of TB pathway genes are upregulated in clinical TB relative to control samples. Fold changes have been converted to a Z-score, with upregulated genes in red and downregulated genes in blue.

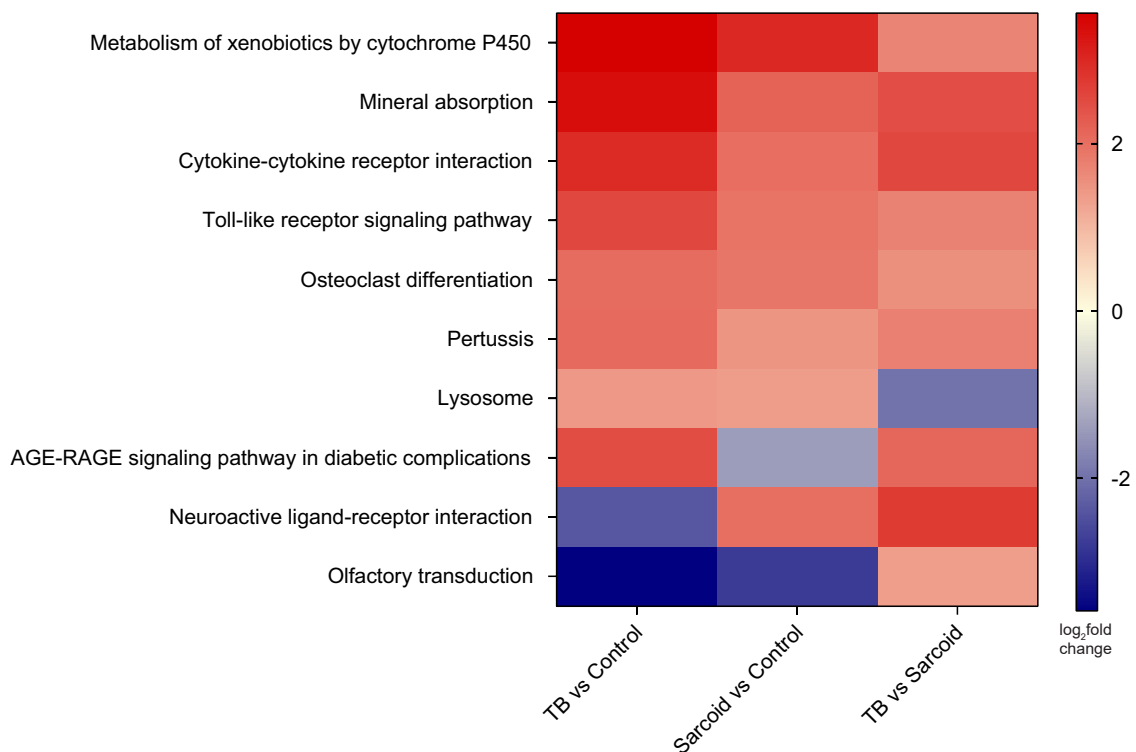


Supplemental Figure 7: Gene ontology analysis of upregulated biological processes in TB relative to sarcoidosis. A) Gene ontology shows the top 20 upregulated biological processes in clinical TB relative to sarcoidosis samples, according to adjusted P value. The cytokine-mediated signaling pathway is the most significantly upregulated biological process in TB. Vertical dashed line indicates adjusted P value 0.05. **B)** Cnetplot of the cytokine-mediated signaling pathway, with each upregulated gene and associated log₂ fold change displayed in TB relative to sarcoidosis, and adjusted P value < 0.05. *MMP1* was the most highly upregulated gene by fold change.

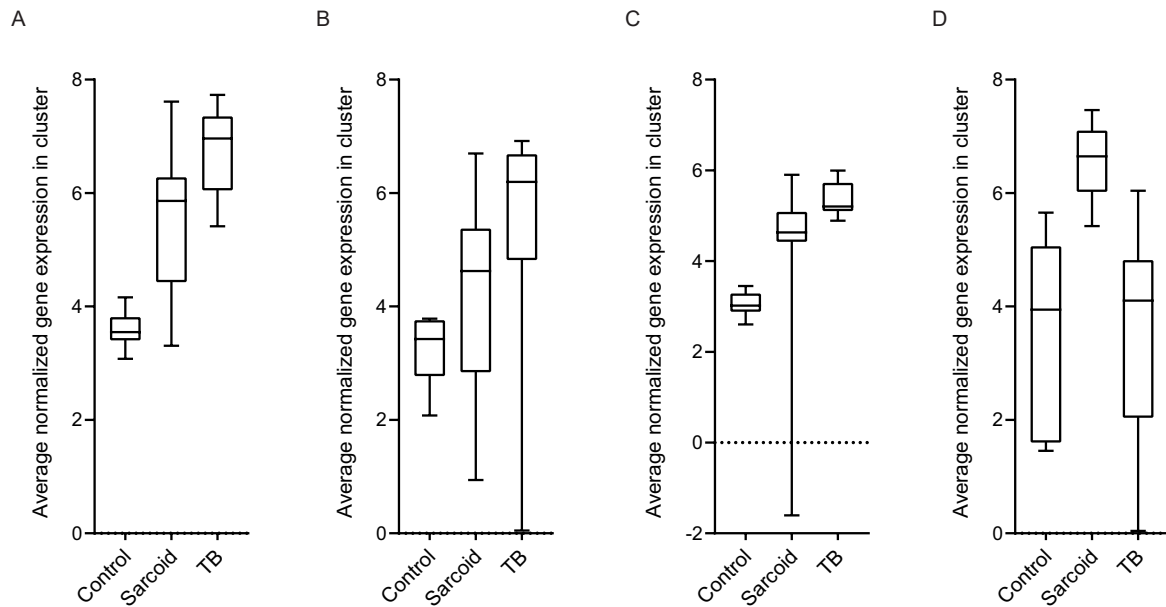
A



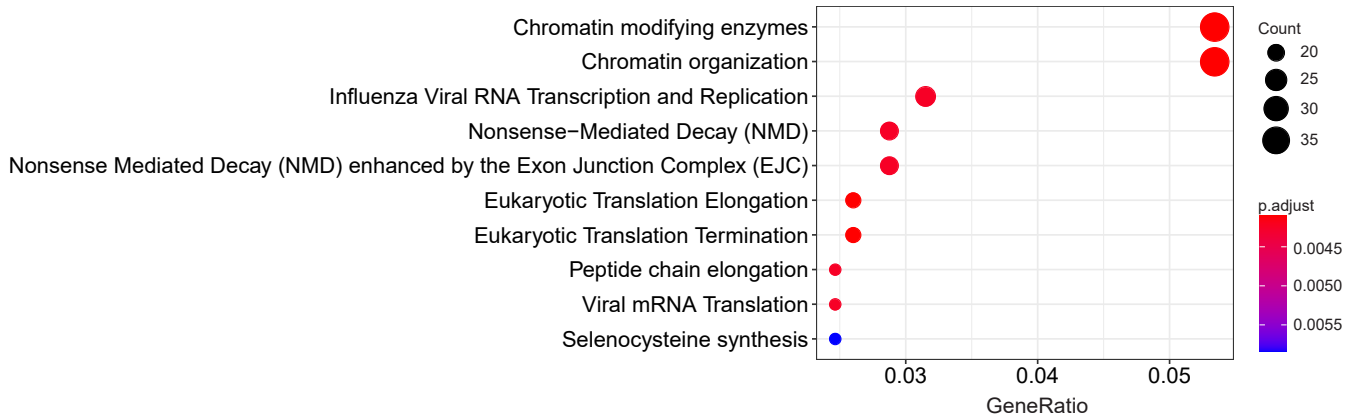
B



Supplemental Figure 8: Gene set enrichment analysis identifies specific differences between TB and sarcoidosis. A) Analysis of the most significant divergently regulated cellular components, according to fold change and adjusted P value, demonstrates the lytic vacuole membrane differentiates TB from sarcoidosis. Adjusted P value < 0.05. **B)** Analysis of the most significant divergently regulated KEGG pathways, according to fold change and adjusted P value, demonstrates the lysosome pathway differentiates TB from sarcoidosis. Adjusted P values are < 0.05.

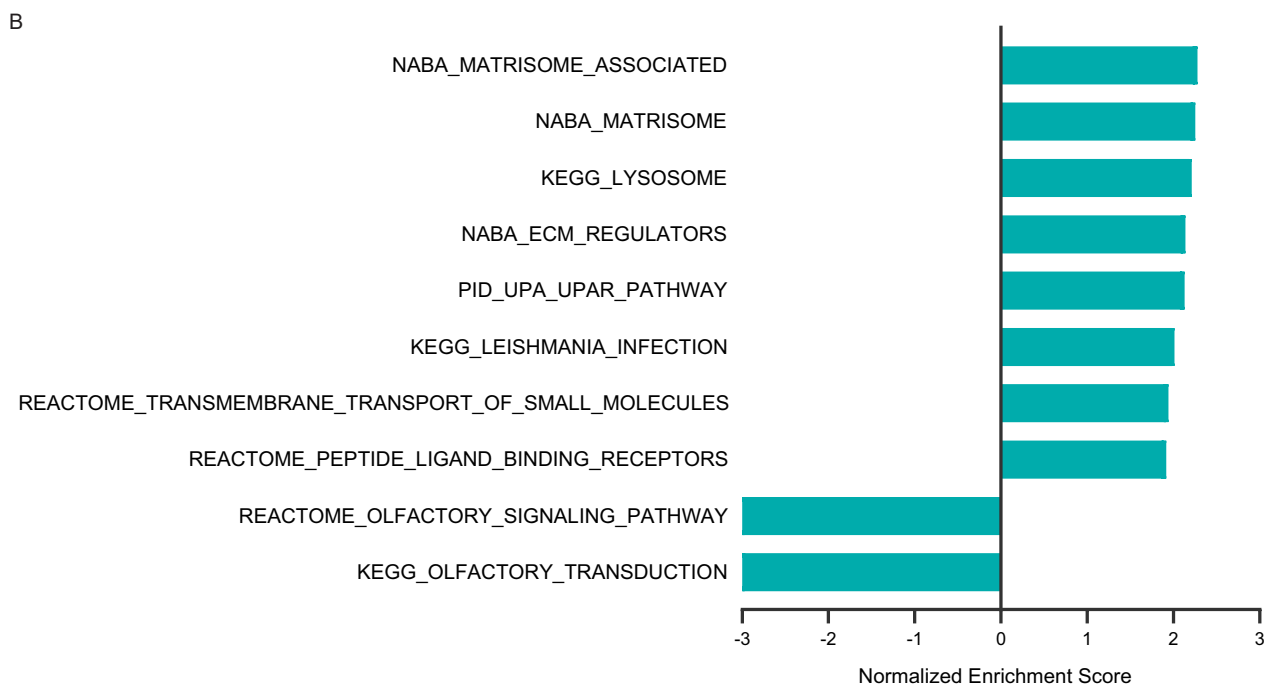
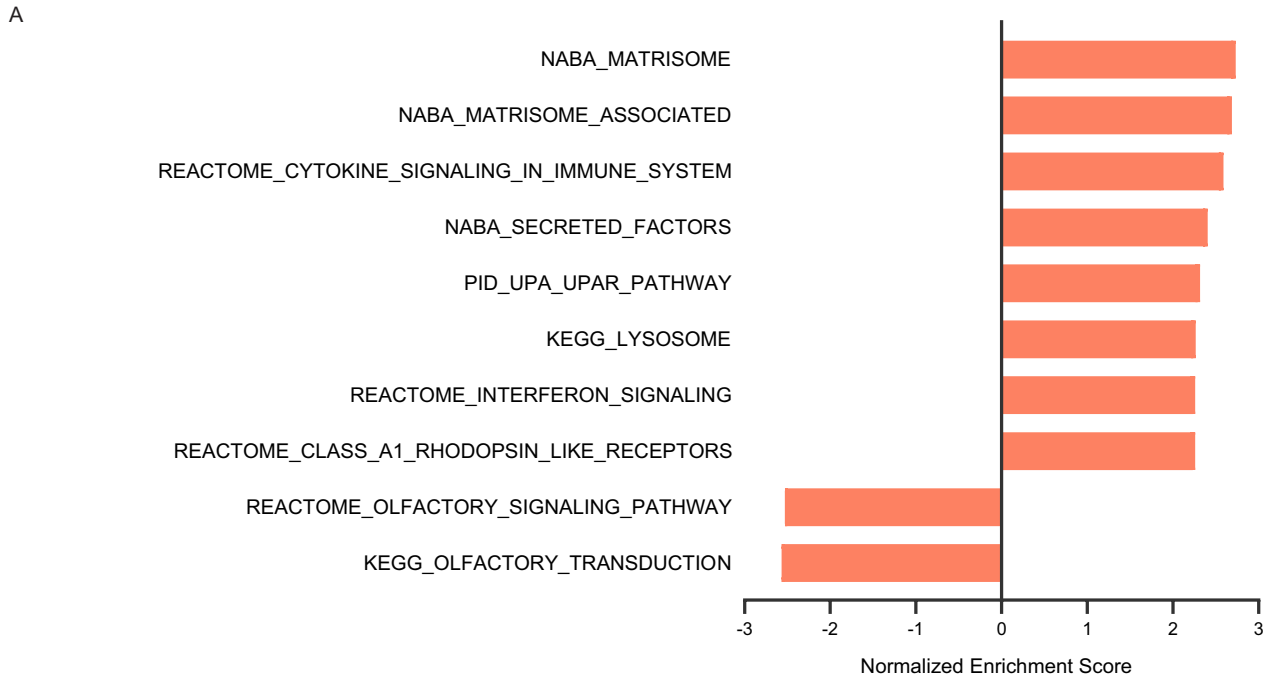


Supplemental Figure 9: Differentiation of clusters predominant in TB or sarcoidosis. Correlation analysis performed utilising Markov Cluster Algorithm (Pearson's R of 0.83) with genes of absolute \log_2 fold change ≥ 1.5 and adjusted P value < 0.05 . Several co-regulated clusters are observed, with those most highly expressed shown for **A**) Cluster 2, **B**) Cluster 7, **C**) Cluster 8, and **D**) Cluster 14. Average (mean) normalized gene expression level, comparing control (n = 7), sarcoidosis (n = 10) and TB samples (n = 7). Gene expression values after TMM normalization used. Box-and-whisker plot with median values (line). Whiskers represent minimum and maximum values, boxes represent the 25th to 75th percentiles. Cluster 14 is the only cluster specific to sarcoidosis and comprises nine genes.



Supplemental Figure 10: Gene ontology analysis of downregulated REACTOME pathways in TB relative to control.

Gene ontology enrichment (ReactomePA program in R, using genes with adjusted P value < 0.05) showing the top 10 downregulated REACTOME pathways in TB relative to control. Chromatin organization and metabolism of RNA and proteins are highly represented. Dot size represents number of expressed genes in the pathway, shade of color represents adjusted P value.

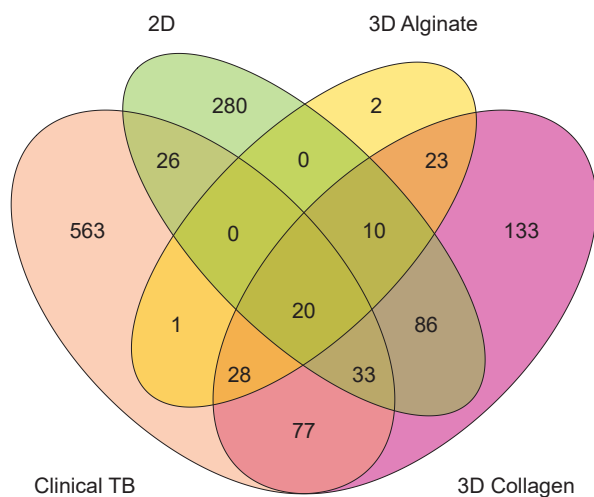


Supplemental Figure 11: Gene set enrichment analysis of clinical TB and sarcoidosis samples. Top 10 canonical pathways according to most extreme normalized enrichment score (NES) in **A)** TB and **B)** Sarcoidosis samples, compared to control samples. Adjusted P values < 0.05.



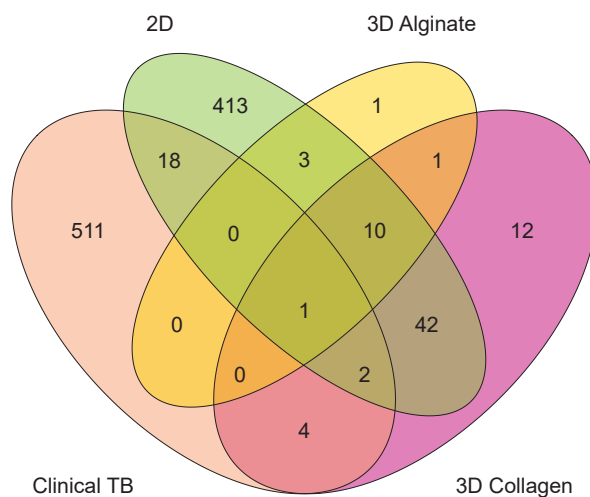
Supplemental Figure 12: Comparison of pathways regulated in lung, lymph node and whole blood of TB patients. Gene ontology enrichment (ReactomePA program in R, using genes with adjusted P value < 0.05) showing the top 10 REACTOME pathways upregulated and downregulated in human TB lung relative to control tissue according to adjusted P value. RNAseq datasets from lung (GSE148036) and whole blood (E-MTAB-7830) were analyzed from raw sequences with the same bioinformatic pipeline used in this current study (Lymph Node), comparing TB to control patients. Pathways are ordered within in each gene ontology category according to adjusted P value (Lung), and gene ontology category is depicted by color. Significant fold change expression for each pathway is depicted. Red: Pathways significantly upregulated in category. Blue: Pathways significantly downregulated in category (adjusted P value < 0.05).

A



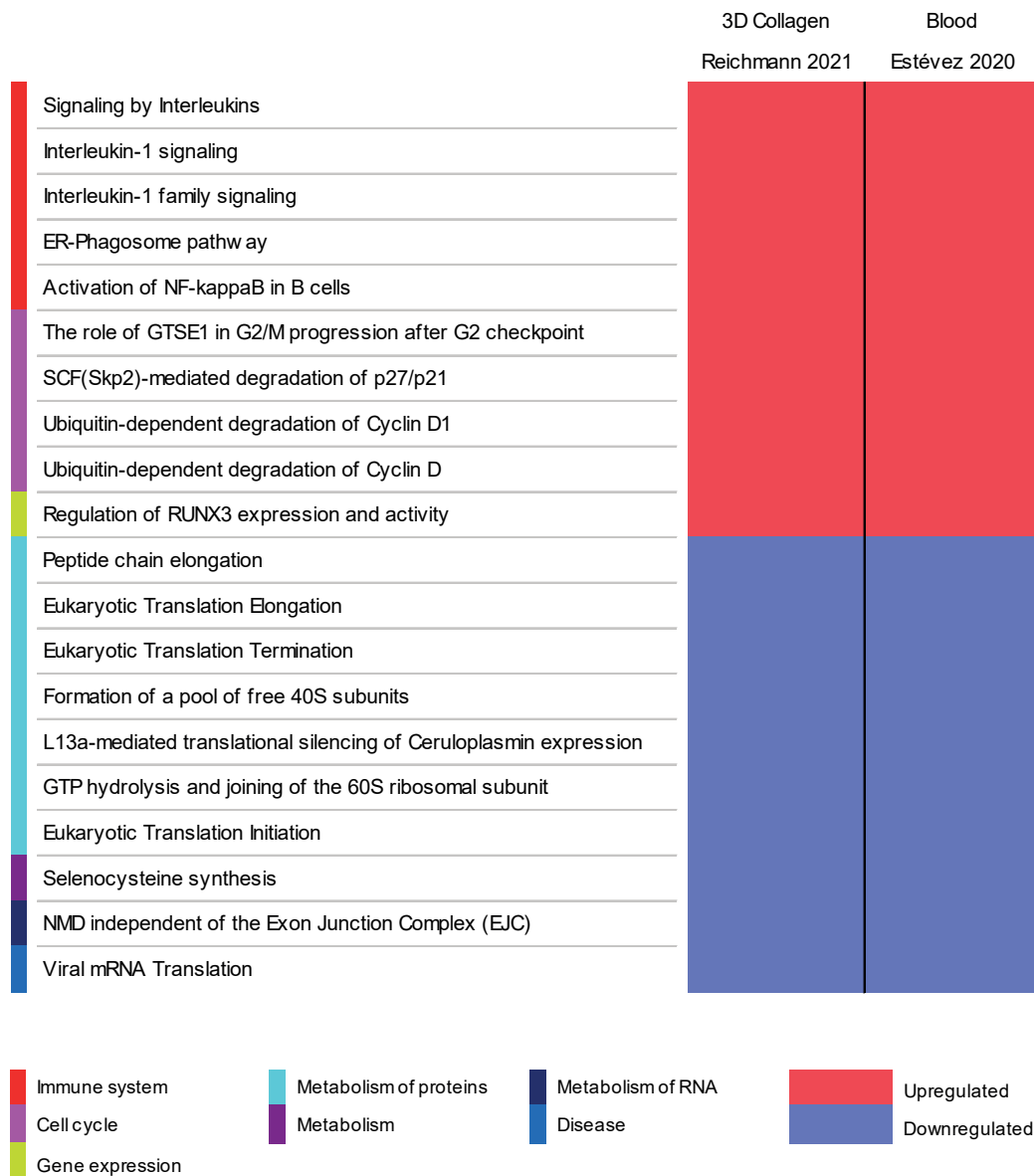
Upregulated

B



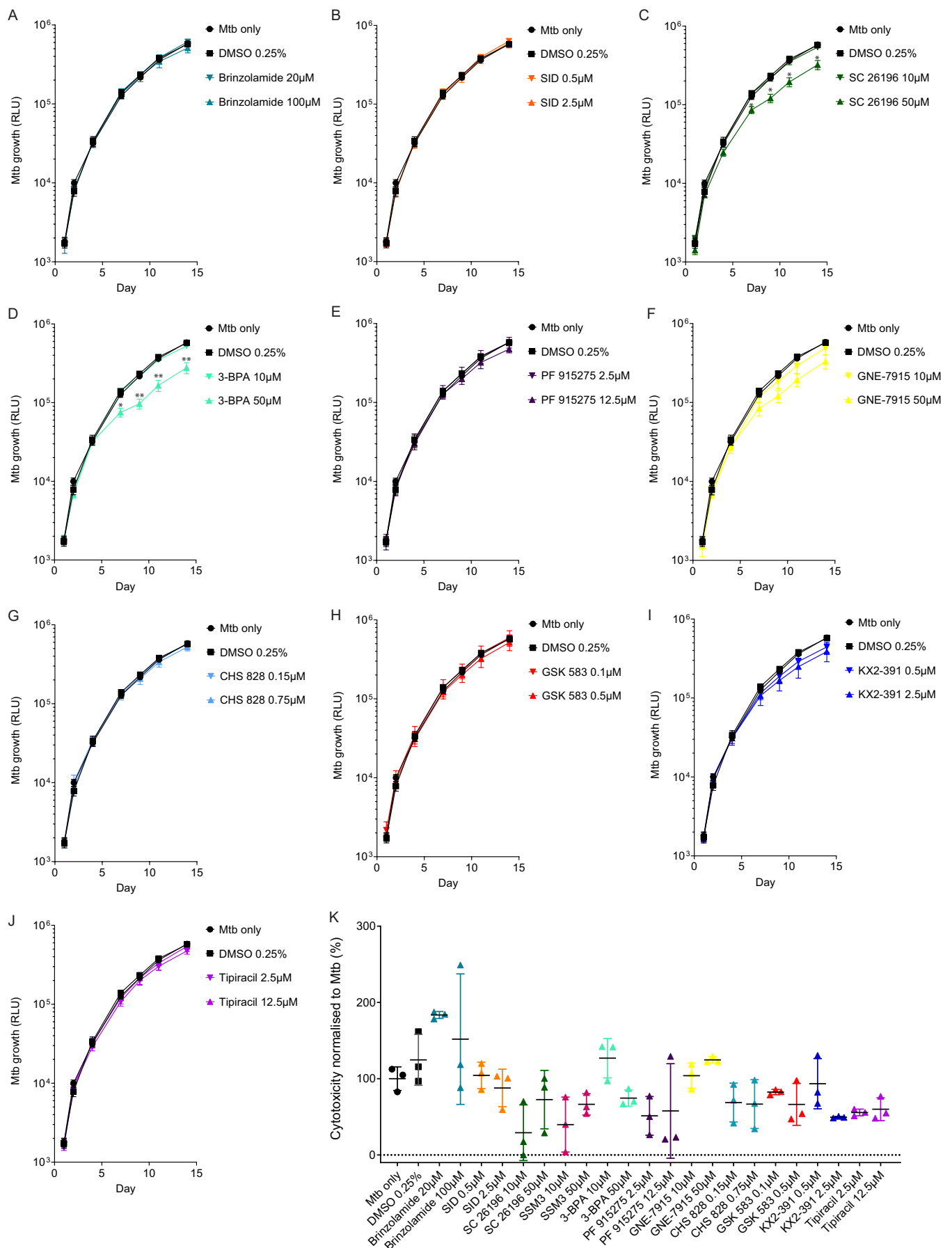
Downregulated

Supplemental Figure 13: Overlap of gene expression in clinical specimens and three human cell culture models. The overlap between upregulated **A)** and downregulated **B)** genes in human TB lymph node biopsies, 2D cell culture, the 3D alginate model and the 3D collagen model was analyzed. Human TB granuloma gene expression was compared to control lymph nodes, while each cell culture analysis compared Mtb infected PBMCs with uninfected PBMCs. Genes with absolute \log_2 fold change ≥ 1.5 with adjusted P value < 0.05 were used in each comparison.

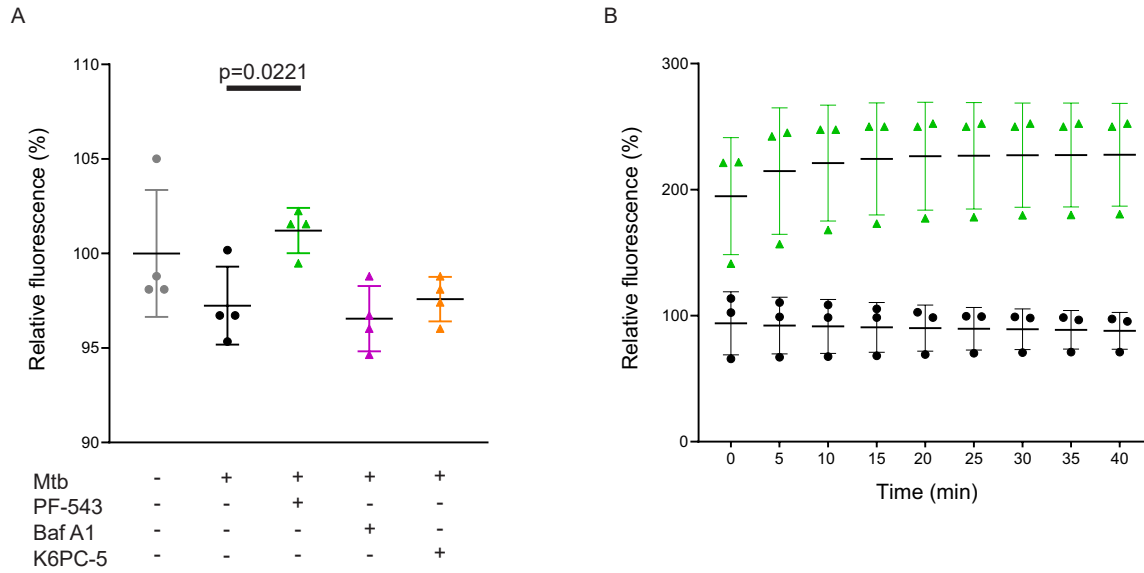


Supplemental Figure 14: Pathways modulated in the 3D collagen model and blood of TB patients closely overlap.

Gene ontology enrichment (ReactomePA program in R, using genes with adjusted P value < 0.05) showing the top 10 REACTOME pathways upregulated and downregulated in the 3D collagen model by Mtb infection, according to adjusted P value. RNAseq dataset from whole blood (E-MTAB-7830) was analyzed from raw sequences with the same bioinformatic pipeline used in this current study (3D Collagen), comparing TB to control patients. Pathways are ordered within in each gene ontology category according to adjusted P value (3D Collagen), and gene ontology category is depicted by color. Significant fold change expression for each pathway is denoted across different cell culture models. Red: Pathways significantly upregulated in category. Blue: Pathways significantly downregulated in category (adjusted P value < 0.05 for each).



Supplemental Figure 15: Host-directed targets with no effect or minor effect in the 3D collagen model. Mtb infected microspheres were treated on day 1 and day 7 with **A)** Brinzolamide, a carbonic anhydrase 2 (CA2) inhibitor, **B)** SID (SID 26681509), a cathepsin L (CTSL) inhibitor, **C)** SC 26196, a fatty acid desaturase 2 (FADS2) inhibitor, **D)** 3-BPA (3-Bromopyruvic acid), a hexokinase 2 (HK2) inhibitor, **E)** PF 915275, a hydroxysteroid 11-beta dehydrogenase 1 (HSD11B1) inhibitor, **F)** GNE-7915, a leucine rich repeat kinase 2 (LRRK2) inhibitor, **G)** CHS 828, a nicotinamide phosphoribosyltransferase (NAMPT) inhibitor, **H)** GSK 583, a receptor interacting serine/threonine kinase 2 (RIPK2) inhibitor, **I)** KX2-391, a SRC proto-oncogene non-receptor tyrosine kinase (SRC) inhibitor, or **J)** Tipiracil, a thymidine phosphorylase (TYMP) inhibitor. Significant suppression of Mtb growth occurred for SC 26196 and 3-BPA, but this was less pronounced than for SphK1 inhibition. Analysis: two way ANOVA, error bars: SD. The same controls are presented in Figure 7A, 7B and Supplemental Figure 15A-J, and all conditions were compared simultaneously against the control by Dunnett's Multiple Comparison Test. **K)** Some inhibitors caused cellular toxicity at the concentrations used. Horizontal bars: mean, error bars: SD. *p<0.05, **p<0.01, ***p<0.001, ****p<0.0001.



Supplemental Figure 16: Sphingosine kinase 1 regulates intracellular pH of monocytes. **A)** Relative fluorescence signal in human monocytes stained with pHrodo taken 5 minutes after Mtb infection (with DMSO 1%), or treated with the SphK1 inhibitor PF-543 50µM, the lysosomal inhibitor Bafilomycin A1 10nM and the SphK1 activator K6PC-5 10µM. Increased fluorescence signal indicates lower pH. Normalized data shown from one donor, analyzed by paired t test. Horizontal bars: mean, error bars: SD. **B)** Relative fluorescence signal in human monocytes stained with LysoSensor taken at 5 minute intervals after Mtb infection for 40 minutes, treated with DMSO 0.1% (black circles) and PF-543 50µM (green triangles). Normalized data shown from one donor. Horizontal bars: mean, error bars: SD.